The predictive content of Spectral Causal Theory

David Alfyorov ·

Independent

CITE AS
openxiv:gr-qc.2026.00003
ISSN
3120-9556 (online)
LICENSE
CC-BY-4.0

POSTED
2026-05-21
VERSION
v1
SUBJECT
gr-qc (+2 cross-listed)

AI DISCLOSURE
ASSISTANT

COVER EVIDENCE

TRANSPARENCY · partial | IDENTITY · strong | PROVENANCE · strong | CITATIONS · partial | MATH · partial | INTEGRITY · partial

The predictive content of Spectral Causal Theory

David Alfyorov

davidich.alfyorov@gmail.com

Abstract

We catalog the predictions of Spectral Causal Theory (SCT), a one-loop gravitational effective field theory derived from the spectral action $S = \mathrm{Tr}(f(D^2/\Lambda^2))$ of a noncommutative spectral triple encoding the Standard Model. Predictions are classified as cutoff-independent (depending only on the Seeley–DeWitt a_4 coefficient) or cutoff-dependent (sensitive to the shape of the cutoff function f). The cutoff-independent sector contains the Weyl-squared coefficient $\alpha_C = 13/120$, the ratio $c_1/c_2 = -1/3$ (frozen under matter-only one-loop RG flow at conformal coupling $\xi = 1/6$), the gravitational wave speed $c_T = c$, and the absence of a scalar gravitational mode at $\xi = 1/6$. The logarithmic black hole entropy correction $c_{\log} = 37/24$ is conditional on stated assumptions. Starobinsky inflation is excluded in the standard spectral action because $\alpha_R(\xi = 1/6) = 0$. For black hole quasinormal modes, modal stability is proven analytically ($V > 3f/r^2 > 0$ for $\ell \geq 2$) and frequency shifts are bounded by $\delta\omega/\omega \sim c_2(\omega/\Lambda)^2 \sim 10^{-20}$ for stellar BHs, fifteen orders below LIGO sensitivity; tidal Love numbers $k_2 \neq 0$ (qualitative difference from GR, but unmeasurably small). Comparison with five quantum gravity programs (LQG, AS, CDT, string theory, IDG) across nine quantitative axes identifies three discriminating observables and five falsification criteria.

Contents

1 Introduction

Spectral Causal Theory (SCT) is a gravitational effective field theory constructed from the spectral action principle of Chamseddine and Connes [**?** **?**]. The classical action is $S = \mathrm{Tr}(f(D^2/\Lambda^2))$, where D is the Dirac operator of an almost-commutative spectral triple encoding both gravitational and Standard Model degrees of freedom, Λ is the spectral cutoff, and f is a positive rapidly decreasing function. The one-loop effective action for the full Standard Model spectrum produces a nonlocal gravitational action with entire-function form factors [**?**].

Six preceding papers from this program report results subsequently used here. Paper 1 [**?**] derived the one-loop form factors for all SM spins (274 checks). Paper 2 [**?**] established that SCT passes all solar system and laboratory tests with $\Lambda > 3.53$ meV (332 checks). Paper 3 [**?**] proved the chirality theorem for the a_8 Seeley–DeWitt coefficient: the spin connection generators $\sigma^{rs} = \frac{1}{4}[\gamma^r, \gamma^s]$ commute with the chirality operator γ_5 in four dimensions, rendering the curvature endomorphism $\Omega_{\mu\nu}$ block-diagonal in the chiral basis. This ensures one-loop UV finiteness unconditionally; two-loop — conditionally on two BV axioms verified at one-loop order [**?**]. Paper 4 [**?**] derived the full nonlinear field equations and their FLRW reduction ($c_T = c$ at one-loop level in the Euclidean derivation). Paper 7 [**?**] constructed a parameter-free bridge formula connecting a causal-set observable to the electric Weyl tensor $E_{ij} = C_{0i0j}$ (CJ $= C_0 N^{8/9} E_{ij} E^{ij} T^4$, verified to $N = 15{,}000$). The present paper collects and classifies the predictions that follow from this body of work.

The purpose is threefold. First, we distinguish predictions that depend only on the universal Seeley–DeWitt coefficients (and are therefore independent of the cutoff function f) from those that depend on the full shape of f. Second, we compare SCT predictions quantitatively with five competing quantum gravity programs. Third, we state explicit criteria under which the theory would be contradicted by observation.

Throughout, we state assumptions and verification status for each result. Results are labeled as *proven* (arithmetic identities formally verified in Lean 4; specifically: rational arithmetic of the a_4 coefficients for given SM multiplicities; physical postulates are not formalized), *verified* (numerically confirmed to 100-digit precision by multiple independent methods), *established* (confirmed through independent re-derivation and literature cross-check), or *conditional* (dependent on stated assumptions).

2 The spectral action and its one-loop effective action

2.1 Classical spectral action

The spectral action for a spectral triple $(\mathcal{A}, \mathcal{H}, D)$ with cutoff scale Λ is [**?** **?**]

$$S_{\mathrm{spec}} = \mathrm{Tr}\big(f(D^2/\Lambda^2)\big), \tag{1}$$

where $f\colon \mathbb{R}_+ \to \mathbb{R}_+$ is a positive, smooth, rapidly decreasing function. For the almost-commutative spectral triple encoding the Standard Model [**?**], the asymptotic expansion for $\Lambda \to \infty$ gives [**?**]

$$S_{\mathrm{spec}} \sim \sum_{k \geq 0} f_{2k}\, \Lambda^{4-2k}\, a_{2k}(D^2), \tag{2}$$

where $f_{2k} = \int_0^\infty f(u)\, u^{k-1}\, \mathrm{d}u$ are the moments and a_{2k} are the Seeley–DeWitt coefficients. The first three terms produce:

- a_0: cosmological constant ($\sim \Lambda^4$),
- a_2: Einstein–Hilbert action $\sim \Lambda^2 \int R\sqrt{g}\, \mathrm{d}^4x$,
- a_4: higher-derivative terms proportional to C^2 and R^2.

The coefficients of C^2 and R^2 in a_4 depend on the SM particle content but not on the cutoff function f.

2.2 One-loop form factors

The one-loop effective action contains nonlocal form factors $F_1(\Box/\Lambda^2)$ and $F_2(\Box/\Lambda^2, \xi)$ multiplying $C_{\mu\nu\rho\sigma}C^{\mu\nu\rho\sigma}$ and R^2 respectively [**?** **?**]. For the choice $f(u) = e^{-u}$, these are constructed from the master function

$$\varphi(x) = \int_0^1 e^{-\alpha(1-\alpha)x}\, \mathrm{d}\alpha = \frac{e^{-x/4}\sqrt{\pi}}{\sqrt{x}}\, \mathrm{erfi}\left(\frac{\sqrt{x}}{2}\right), \tag{3}$$

satisfying $\varphi(0) = 1$ and $\varphi'(0) = -1/6$. Figure 1 compares $\varphi_n(x)$ for $n = 1, 2, 3, 5$; the functions share $\varphi_n(0) = 1$ but differ at all $x > 0$.

The per-spin Weyl form factors, expressed as functions of $x = -\Box/\Lambda^2$ (Euclidean momentum squared in units of Λ^2), are [**?** **?**]:

$$h_C^{(0)}(x) = \frac{1}{12x} + \frac{\varphi - 1}{2x^2}, \tag{4}$$

$$h_C^{(1/2)}(x) = \frac{3\varphi - 1}{6x} + \frac{2(\varphi - 1)}{x^2}, \tag{5}$$

$$h_C^{(1)}(x) = \frac{\varphi}{4} + \frac{6\varphi - 5}{6x} + \frac{\varphi - 1}{x^2}, \tag{6}$$

Equations (4)–(6) are derived for the choice $f(u) = e^{-u}$. The algebraic structure (rational functions of x with φ-dependent coefficients) relies on the fact that $\varphi'(0) = -1/6$ cancels the $1/x$ divergence at $x = 0$. For alternative cutoffs $f(u) = e^{-u^n}$ with $n \geq 2$, the master function satisfies $\varphi_n'(0) = 0$, so this cancellation does not occur and the form factors require a separate heat kernel derivation. In Section 4.2 we use the formal substitution $\varphi \to \varphi_n$ in (4)–(6) to estimate the propagator zeros; this is valid at finite z (where no divergence arises) but does not yield a consistent $z \to 0$ limit for $n \geq 2$.

The Dirac form factor (5) evaluates to $h_C^{(1/2)}(0) = -1/20$ (negative): the factor $(3\varphi - 1) \to 2$ and $(\varphi - 1) \to 0$ cancel the $1/x$ terms leaving a negative finite limit. This sign encodes the fermionic functional trace [**?**].

The total SM Weyl coefficient is

$$\alpha_C(x) = N_s\, h_C^{(0)}(x) + N_D\, h_C^{(1/2)}(x) + N_v\, h_C^{(1)}(x), \tag{7}$$

with SM multiplicities $N_s = 4$ (real Higgs scalars), $N_D = N_f/2 = 22.5$ (Dirac fermions), $N_v = 12$ (gauge vectors) [**?**]. At $x = 0$, using $h_C^{(0)}(0) = +1/120$, $h_C^{(1/2)}(0) = -1/20$, $h_C^{(1)}(0) = +1/10$:

$$\alpha_C(0) = 4 \cdot \frac{1}{120} + 22.5 \cdot \left(-\frac{1}{20}\right) + 12 \cdot \frac{1}{10} = \frac{13}{120}. \tag{8}$$

This value depends only on the SM particle content and is independent of the cutoff function f. The count $N_f = 45$ Weyl fermions is the standard SM without right-handed neutrinos, following [**?**]. The Chamseddine–Connes spectral triple [**?**] includes right-handed neutrinos with Majorana mass; their inclusion would modify α_C. A detailed treatment of the Majorana contribution is beyond the scope of this paper.

2.3 Modified propagator and the fakeon prescription

The one-loop effective action for quantum fields on a curved background has the universal form [**?** **?**]

$$\Gamma^{(1)} = \frac{1}{16\pi^2}\int \mathrm{d}^4x\sqrt{g}\,\big[C_{\mu\nu\rho\sigma}F_1(\Box/\Lambda^2)\,C^{\mu\nu\rho\sigma} + R\,F_2(\Box/\Lambda^2,\xi)\,R\big], \tag{9}$$

where F_1, F_2 are nonlocal form factors. Linearization around flat space $g_{\mu\nu} = \eta_{\mu\nu} + h_{\mu\nu}$ and the Barnes–Rivers decomposition into projectors $P^{(2)}$ (tensor, spin-2, 5 components) and $P^{(0-s)}$ (scalar, 1 component) give the inverse propagator [**?**]

$$G^{-1}_{\mu\nu,\rho\sigma}(k) = k^2\big[\Pi_{\mathrm{TT}}(z)\,P^{(2)}_{\mu\nu,\rho\sigma} + \Pi_s(z,\xi)\,P^{(0-s)}_{\mu\nu,\rho\sigma}\big], \tag{10}$$

where $z = k^2/\Lambda^2$ and

The dressed spin-2 propagator denominator is [**?** **?**]

$$\Pi_{\mathrm{TT}}(z) = 1 + c_2\,z\,\hat{F}_1(z), \tag{11}$$

where $c_2 = 2\alpha_C = 13/60$, $z = k^2/\Lambda^2$, and $\hat{F}_1(z) = F_1(z)/F_1(0)$ is the normalized shape function ($\hat{F}_1(0) = 1$), with $F_1(z) = \alpha_C(z)/(16\pi^2)$ from (7). For $f = e^{-u}$, Π_{TT} has its first positive real zero at

$$z_0 = 2.4148, \qquad m_2 = \sqrt{z_0}\,\Lambda = 1.554\,\Lambda\,. \tag{12}$$

This zero corresponds to a massive mode treated via the fakeon prescription [**?** **?**] (building on the Lee–Wick framework [**?**]): the mode does not appear in asymptotic states and contributes only through virtual exchange. The fakeon prescription is formulated for propagators with finitely many poles; its extension to the SCT propagator, which as an entire function of order 1 has countably many complex zeros, requires a convergence proof not provided here. Unitarity under this prescription has been verified at one loop [**?**]; the all-orders proof requires extending Anselmi's finite-threshold argument to infinitely many poles.

The Stelle Lagrangian mass [**?**] $m_{\mathrm{Stelle}} = \Lambda/\sqrt{c_2} = \Lambda\sqrt{60/13} \approx 2.148\,\Lambda$ differs from the propagator pole mass (12) because the nonlocal form factor $\hat{F}_1(z)$ modifies the zero position relative to the local approximation $\Pi_{\mathrm{TT}} \approx 1 + c_2 z$.

The scalar mode propagator is

$$\Pi_s(z,\xi) = 1 + 6(\xi - \tfrac{1}{6})^2\,z\,\hat{F}_2(z,\xi). \tag{13}$$

At $\xi = 1/6$: $\Pi_s = 1$ identically, and the scalar mode decouples.

2.4 The cutoff function f

The function f in (1) is constrained but not uniquely determined by the spectral action principle. Entire-function form factors (required for the absence of propagator branch cuts) demand that $f(u)$ extend to an entire function of the complex variable u. The family $f(u) = e^{-u^n}$ for $n \in \mathbb{N}$ satisfies this constraint; non-integer powers (e.g., $e^{-u^{3/2}}$) produce branch cuts at $u = 0$ and are excluded.

Different choices of n give different master functions

$$\varphi_n(x) = \int_0^1 \exp\bigl(-[\alpha(1-\alpha)\,x]^n\bigr)\,\mathrm{d}\alpha, \tag{14}$$

different form factors, and different propagator zeros. The a_4 coefficient $\alpha_C(0) = 13/120$ is independent of n.

3 Cutoff-independent predictions

The predictions in this section depend only on the Seeley–DeWitt coefficient a_4 and its evaluation on specific backgrounds. They are independent of the cutoff function f and constitute the core predictive content of SCT.

Table 1: Cutoff-independent predictions. Status levels: *proven* = arithmetic identity verified in Lean 4 (formalized: rational arithmetic of a_4 coefficients for given SM multiplicities; physical postulates not formalized); *verified* = confirmed numerically to 100-digit precision by independent methods; *established* = confirmed through independent re-derivation and literature cross-check; *conditional* = dependent on stated assumptions.

Prediction	Value	Source	Status
α_C (Weyl^2 coeff.)	$13/120$	[**?**]	proven
c_1/c_2 at $\xi = 1/6$	$-1/3$	[**?**]	proven
γ_{PPN}, β_{PPN}	$1 + \mathcal{O}(e^{-10^{14}})$	[**?**]	conditional†
c_T (GW speed)	c (one-loop, Euclidean derivation)	[**?**]	conditional†
$c_{\log}$ (BH entropy)	37/24 (SM); 8/5 (SM+ν_R)	App. B	conditional‡
Scalar grav. mode	absent at $\xi = 1/6$	[**?** **?**]	established
Starobinsky inflation	excluded in std. NCG	Sec. 3.5	established

†Conditional on the generalized fakeon prescription for a propagator with infinitely many complex zeros (convergence proof open).

‡Conditional on: (a) the Sen formula with graviton contribution +424 (ensemble zero-mode corrections: Sen [**?**], Section 4.2: $\delta c_{\log} \in [-3/4, 0]$ for non-extremal BHs); (b) SM field content ($N_F = 22.5$ includes ν_R via spectral triple [**?**]; without ν_R: $c_{\log} = 89/60$, ∼4% change). The *sign* $c_{\log} > 0$ is robust to both sources of uncertainty and discriminates against LQG ($c_{\log}^{\mathrm{LQG}} < 0$).

Remark 3.1 (Bridge formula). The CJ (curvature junction) bridge formula of [**?**], $\langle \mathrm{CJ} \rangle = C_0 N^{8/9} E_{ij} E^{ij} T^4$ with $C_0 = 32\pi^2/(3 \cdot 9! \cdot 45)$, relates a stratified covariance estimator on a Poisson-sprinkled causal set (N elements, diamond proper time T) to the electric Weyl

tensor $E_{ij} = C_{0i0j}$. This is an additional cutoff-independent prediction for causal-set observables. It is not included in Table 8 because it is not directly testable by continuum-spacetime experiments.

3.1 The Weyl coefficient α_C

The value $\alpha_C = 13/120$ follows from (8) and depends only on the SM particle content counted in the a_4 heat kernel coefficient. It is independent of the cutoff function f, since a_4 is a universal coefficient in the heat kernel expansion (2). The value has been formally verified in Lean 4 and cross-checked against three independent literature sources [**?** **?** **?**] (source code in [**?**]). 354 numerical checks pass at 100-digit precision.

3.2 RG stability of c_1/c_2

The local part of the one-loop effective action (9) contains two curvature-squared invariants: $\Gamma^{(1)}_{\rm loc} = \int (c_1\, C_{\mu\nu\rho\sigma}C^{\mu\nu\rho\sigma} + c_2\, R^2)\sqrt{g}\,\mathrm{d}^4x$, where c_1 and c_2 are the coefficients of C^2 and R^2. In the Shapiro normalization [**?**] (without the $1/(16\pi^2)$ prefactor): $c_1 = -2\alpha_C/3$, $c_2 = 2\alpha_C$. In the (9) normalization (with the $1/(16\pi^2)$ prefactor): $c_1 = F_1(0) = \alpha_C/(16\pi^2)$. The ratio c_1/c_2 is normalization-independent.

At conformal coupling $\xi = 1/6$ (the value predicted by the spectral triple; see Section 3.4):

$$c_1 = -\frac{2\alpha_C}{3} = -\frac{13}{180}\,, \qquad c_2 = 2\alpha_C = \frac{13}{60}\,, \qquad \frac{c_1}{c_2} = -\frac{1}{3}\,. \tag{15}$$

The one-loop matter beta functions are

$$\beta_{c_2} = \frac{2\alpha_C}{(4\pi)^2} = 1.372\times10^{-3}\,, \qquad \beta_{c_1} = -\frac{2\alpha_C}{3(4\pi)^2} = -4.574\times10^{-4}\,. \tag{16}$$

Because $\beta_{\alpha_R} = 0$ at $\xi = 1/6$ (this coupling is a fixed point of the one-loop RG), the ratio

$$\frac{\beta_{c_1}}{\beta_{c_2}} = -\frac{1}{3} \quad \text{(algebraic identity at } \xi = 1/6\text{)}. \tag{17}$$

Consequently, $c_1(t)/c_2(t) = -1/3$ for all $t = \ln(\mu/\Lambda)$ along the matter-only one-loop trajectory.

Table 2: Running couplings $c_1(\mu)$ and $c_2(\mu)$ along the matter-only one-loop trajectory, with initial conditions at $\mu = \Lambda$.

μ/Λ	t	c_1	c_2	c_1/c_2
1	0	−0.07222	0.21667	−1/3
10^{-1}	−2.303	−0.07117	0.21351	−1/3
10^{-5}	−11.513	−0.06696	0.20087	−1/3
10^{-10}	−23.026	−0.06169	0.18507	−1/3
10^{-20}	−46.052	−0.05116	0.15348	−1/3

The SCT ratio $c_1/c_2 = -0.333$ differs from the perturbative asymptotic freedom branch (-0.326; [**?**]) by 2% and from the Reuter non-Gaussian fixed point (-1.09, truncation-dependent; [**?**]) by a factor of 3.3.

3.3 Black hole entropy

The logarithmic correction to the Bekenstein–Hawking entropy is

$$S = \frac{A}{4G} + c_{\log} \ln \frac{A}{\ell_P^2} + \mathcal{O}(1), \tag{18}$$

where the coefficient $c_{\log} = 37/24 \approx 1.54$ (SM field content; with ensemble zero-mode uncertainty $\delta c_{\log} \in [-3/4, 0]$; sign robust) follows from the Sen formula [**?**], Section 4.2 (Appendix B). The formula uses zeta-function regularisation on the Euclidean Schwarzschild instanton with Dirichlet boundary conditions at the horizon. The result depends on the fermion count $N_F = 22.5$ Dirac (without right-handed neutrinos; see Section 2.2) and on the graviton contribution +424 (gauge-invariant, determined by the one-loop determinant on the Euclidean Schwarzschild instanton).

The *sign* of $c_{\log}$ discriminates between programs: SCT gives $c_{\log} > 0$ (value 37/24 for SM content, 8/5 for SM+ν_R; both positive). LQG robustly predicts $c_{\log} < 0$: $-1/2$ [**?**] or $-3/2$ [**?**] depending on the method. The discriminator is the sign, not the precise numerical value, since the latter depends on the ensemble choice and field content. In asymptotic safety, the result is definition-dependent: 0 for thermodynamic entropy or π/g_* for Clausius entropy [**?**]. IDG produces no logarithmic correction (power-law only) [**?**].

3.4 Absence of scalar gravitational mode

The non-minimal Higgs–gravity coupling ξ is determined by the spectral triple. In the standard Chamseddine–Connes spectral action, the a_4 coefficient contains a common Yukawa-dependent factor multiplying both the curvature coupling $R|H|^2$ and the kinetic term $|\nabla H|^2$. After canonical normalization, this gives $\xi = 1/6$ (conformal coupling). This has been confirmed in five independent works [**?** **?** **?** **?** **?**]. At $\xi = 1/6$, the RG beta function $\beta_\xi \propto (\xi - 1/6)$ [**?**] vanishes, so $\xi = 1/6$ is an exact one-loop fixed point.

At $\xi = 1/6$: $\alpha_R = 2(\xi - 1/6)^2 = 0$ and $\Pi_s = 1$ identically (13). This is a consequence of the conformal invariance of massless fermions and gauge bosons in $d = 4$: their one-loop R^2 beta functions vanish ($\beta_R^{(1/2)} = \beta_R^{(1)} = 0$), and only scalars ($\beta_R^{(0)} = \frac{1}{2}(\xi - \frac{1}{6})^2$) contribute to α_R. At $\xi = 1/6$ the scalar contribution also vanishes. The scalar gravitational mode does not propagate. Consequence: exactly two gravitational wave polarizations (tensor modes only).

All known BSM scalars arising from NCG spectral triples also acquire $\xi' = 1/6$, because the same Yukawa-factor mechanism applies to any scalar from the finite Dirac operator [**?** **?** **?**].

Detection of a scalar gravitational wave polarization would imply $\xi \neq 1/6$, requiring modification of the standard spectral triple.

3.5 Exclusion of Starobinsky inflation

Since $\alpha_R = 0$ at $\xi = 1/6$, the R^2 term in the effective action is absent. There is no scalaron. Starobinsky inflation, which requires a propagating R^2 scalar with mass $M_{\rm inf} \approx 1.28 \times 10^{-5}\, M_P$, is excluded in the standard spectral action.

The only path not definitively excluded is reinterpretation of Λ as a sub-Planckian intermediate scale, or framework extension (zeta spectral action [**?**], dilatonized action [**?**]). These require departing from the standard Chamseddine–Connes spectral action. No symmetry argument is known that would protect $\alpha_R = 0$ beyond one loop.

Table 3: Mechanisms for reducing the scalaron mass to $M_{\rm inf}$, and why each fails within the standard NCG spectral action.

Mechanism	$M_0/M_{\rm inf}$	Obstruction
Sub-Planckian Λ	~ 1	Conflicts with GUT interpretation of Λ
Large $\xi \sim 2 \times 10^4$	~ 1	Violates spectral-triple geometric BC
NCG σ-singlet [**?**]	unchanged	$\xi_\sigma = 1/6$ (conformal)
Pati–Salam [**?**]	unchanged	All scalars conformal
Grand Symmetry [**?**]	unchanged	σ for Higgs mass, not scalaron
Many BSM scalars ($\xi' = 0$)	~ 1	Requires $N_s' \sim 4 \times 10^{10}$
Two-loop corrections	unknown	No published calculation
Modified $f(u)$	cannot help	α_R from a_4, independent of f

4 Cutoff-dependent predictions

The predictions in this section depend on the full shape of the cutoff function f through the master function $\varphi_n(x)$ (14). They are *not* uniquely predicted without an additional principle fixing f.

4.1 The cutoff function constraint

The requirement that the form factors F_1, F_2 be entire functions of $z = \Box/\Lambda^2$ restricts the class of admissible cutoff functions. For the family $f(u) = e^{-u^\alpha}$, entireness holds if and only if $\alpha \in \mathbb{N}$ (positive integer). At non-integer α (e.g., $\alpha = 3/2$), the function u^α has a branch point at $u = 0$, and the resulting form factors inherit branch cuts. Power-law cutoffs $f(u) = (1+u)^{-N}$ are likewise excluded.

The conventional choice $f(u) = e^{-u}$ ($n = 1$) is computationally convenient but not uniquely determined. The choices e^{-u^2}, e^{-u^3}, etc., are equally admissible.

4.2 Cutoff function scan

To illustrate the sensitivity of cutoff-dependent predictions to the choice of f, we compute the propagator zeros by formally substituting $\varphi \to \varphi_n$ in the form factors (4)–(6). This substitution is evaluated at finite z (the propagator zeros lie at $z_0 > 2$, far from the $z \to 0$ divergence that arises for $n \geq 2$; see Section 2.2). Table 4 reports the results for $n \in \{1, \ldots, 5\}$.

For $n \geq 2$, the fakeon mass lies in the range $m_2/\Lambda \in [2.274, 2.291]$ (spread 0.7%). The $n = 1$ (exponential) cutoff is an outlier at $m_2/\Lambda = 1.554$; the exponential form factor changes sign at a lower value of z than the sharper ($n \geq 2$) cutoffs, pulling the propagator zero closer to the origin.

The Stelle Lagrangian mass $m_{\rm Stelle} = \Lambda\sqrt{60/13} \approx 2.148\,\Lambda$ (from the local approximation $\Pi_{\rm TT} \approx 1 + c_2 z$) differs from all five pole masses in Table 4 because the nonlocal form

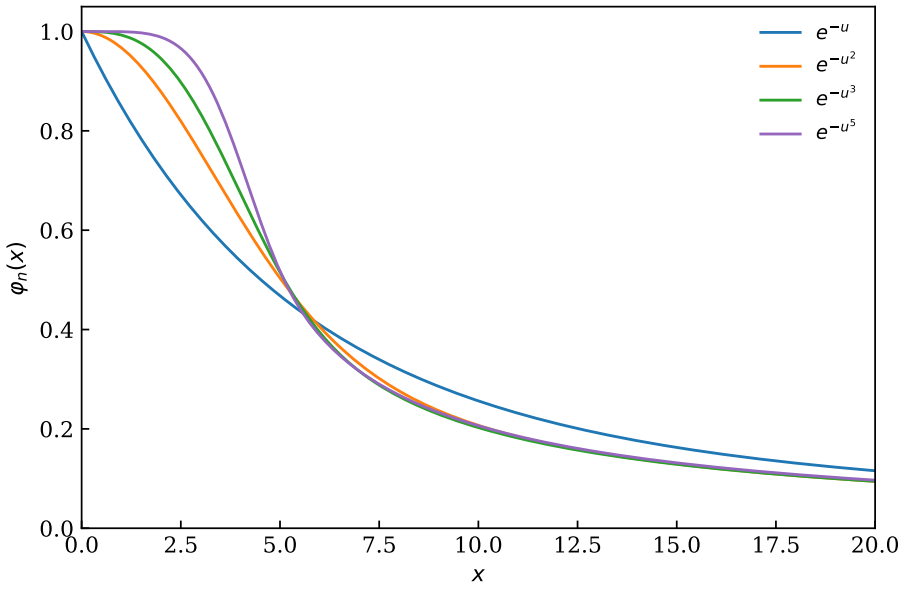

Figure 1: Master functions $\varphi_n(x)$ for the cutoff family $f(u) = e^{-u^n}$. All share $\varphi_n(0) = 1$ (the cutoff-independent IR limit) but differ at $x > 0$. The exponential cutoff ($n = 1$) decays most slowly; sharper cutoffs ($n \geq 2$) produce steeper descent and converge toward a common profile.

factor modifies the zero position.

4.3 Modified Newtonian potential

At $\xi = 1/6$ (scalar mode absent), the modified Newtonian potential takes the single-Yukawa form. In the static limit, the Fourier transform of the propagator (10) gives $V(r) \propto \int \mathrm{d}^3k\, e^{i\mathbf{k}\cdot\mathbf{r}}/[k^2\Pi_{\mathrm{TT}}(k^2/\Lambda^2)]$. The residue of the spin-2 pole at $\Pi_{\mathrm{TT}}(z_0) = 0$ is $R_0 = 1/[z_0\Pi'_{\mathrm{TT}}(z_0)] < 0$ (negative, since Π_{TT} crosses zero from above). The coefficient $-4/3$ arises from the weight of the $P^{(2)}$ projector in the tensor structure of the inverse propagator (10):

$$\frac{V(r)}{V_N(r)} = 1 - \frac{4}{3}\, e^{-m_2 r}, \tag{19}$$

where $m_2 = \sqrt{z_0}\,\Lambda$ is the fakeon mass from Table 4. In the Yukawa approximation, $V(0)/V_N = -1/3$ (repulsive at the origin). This is an artifact of the local approximation: the full nonlocal potential, defined by the Fourier integral of $1/\Pi_{\mathrm{TT}} - 1$, diverges as $r \to 0$, since $1/\Pi_{\mathrm{TT}} - 1 \to -1$ as $z \to \infty$. The Yukawa approximation is valid for $r \gg 1/\Lambda$.

At solar system distances ($r \sim 1$ AU), with $\Lambda > 3.53$ meV. This bound is obtained as follows: at $\xi = 1/6$ the scalar mode is absent (Section 3.4), and the potential (19) has a single Yukawa term with the nonlocal mass $m_2 = 1.554\,\Lambda$ (12). The Eöt-Wash experiment [**?**] constrains the Yukawa correction $|\alpha|\, e^{-r/\lambda}$ at $\lambda = 1/m_2 = 1/(1.554\,\Lambda)$ and $|\alpha| = 4/3$, giving $\Lambda > 3.53$ meV (update of the bound [**?**], previously obtained in the two-component Stelle parametrization): $m_2 r \sim 10^8$ and $V/V_N = 1 - (4/3)\, e^{-10^8} = 1$ to exponential precision.

Table 4: Cutoff function scan for $f(u) = e^{-u^n}$. Here z_0 is the first positive real zero of $\Pi_{\rm TT}(z)$, obtained by formal substitution $\varphi \to \varphi_n$ in (4)–(6), and $V(1)/V_N$ is the modified Newtonian potential at $r\Lambda = 1$. For all n, $\alpha_C(0) = 13/120$ (cutoff-independent). The zeros z_0 are computed at finite z where the formal substitution is well-defined; the $z \to 0$ limit diverges for $n \geq 2$ (see text). This family does not exhaust all admissible cutoff functions; wider families could produce values outside the shown range.

n	$x \cdot \varphi_n(x \to \infty)$	z_0	m_2/Λ	$V(1)/V_N$
1	2.00	2.415	1.554	0.718
2	1.77	5.174	2.274	0.863
3	1.79	5.248	2.291	0.865
4	1.81	5.229	2.287	0.865
5	1.84	5.208	2.282	0.864

4.4 Graviton dispersion relation

The linearized equation of motion for tensor perturbations is $\Pi_{\rm TT}(\Box/\Lambda^2)\,\Box\, h_{\mu\nu} = 0$, which in momentum space becomes $\Pi_{\rm TT}(z) \cdot z = 0$ with $z = (-\omega^2 + k^2)/\Lambda^2$. This factors into two branches:

(i) $z = 0$, i.e., $\omega^2 = k^2$: the massless graviton with $v_{\rm ph} = v_g = c$. This mode is unmodified because $\Pi_{\rm TT}$ is a scalar multiplicative factor acting on the Lorentz-invariant combination k^2.

(ii) $\Pi_{\rm TT}(z_0) = 0$: massive fakeon modes. These do not propagate as physical particles under the fakeon prescription.

The massless graviton dispersion relation ($z = 0$ branch) is $\omega^2 = k^2$ exactly at one loop: there is no birefringence, and the signal velocity equals c. This is a result about free propagation on flat background; on curved backgrounds (e.g., Schwarzschild), the perturbation equation acquires corrections $\sim c_2(\omega/\Lambda)^2$ from the nonlocal form factor — see Section 5.2. Both statements (Euclidean derivation) are conditional on the correctness of the Wick rotation for form factors F_1 that are entire functions of the complex argument.

This is compatible with the GW170817 bound [**?**] $|c_T - c|/c < 10^{-15}$, which SCT satisfies exactly (not approximately) at one loop.

5 What SCT does not predict

5.1 No cosmological constant prediction

The cosmological constant $\Lambda_{\rm cc}$ enters the spectral action through the a_0 coefficient and the moment $f_4 = \int_0^\infty f(u)\, u\, {\rm d}u$ (in the Chamseddine–Connes convention where $a_0 \propto f_4\, \Lambda^4$). The physical value of $\Lambda_{\rm cc}$ is not predicted; it is a free parameter set by the choice of f_4 and the renormalization-group trajectory. The spectral action generically produces $a_0 \propto f_4 \Lambda^4$, which exceeds the observed $\Lambda_{\rm cc} \sim 10^{-122}\, M_P^4$ by ~ 120 orders of magnitude; SCT inherits the cosmological constant problem from quantum field theory. This gap is shared by LQG, AS, and IDG.

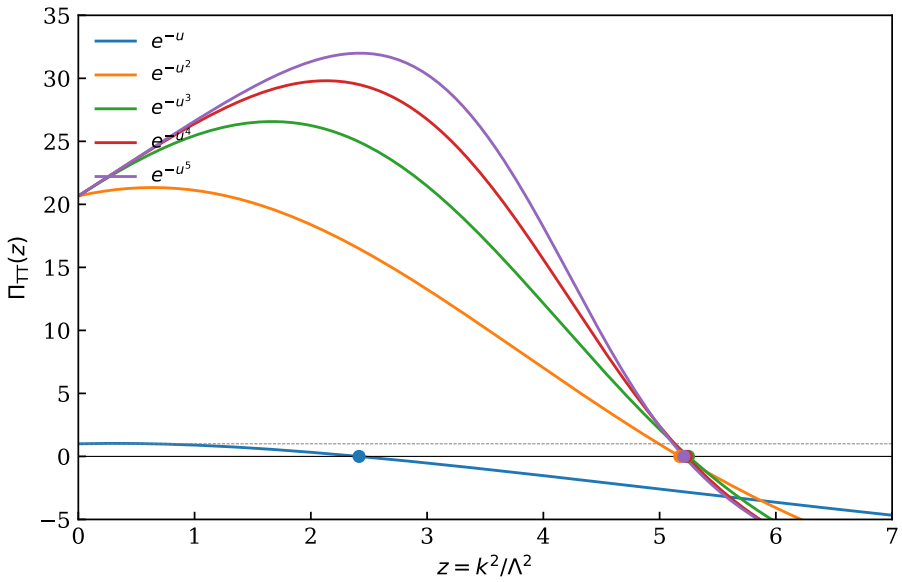

Figure 2: The dressed propagator denominator $\Pi_{\mathrm{TT}}(z)$ for five cutoff functions. Circles mark the first positive real zero z_0 (the fakeon pole). The exponential cutoff ($n = 1$) crosses zero at $z_0 = 2.41$; the sharper cutoffs ($n \geq 2$) cross near $z_0 \approx 5.2$.

5.2 Black hole quasinormal modes

QNM frequency shifts in SCT receive two independent contributions:

1. *Metric modification* (Level 2, computed): $\delta\omega/\omega \sim \exp(-m_2 r_{\mathrm{peak}})$. For GW150914 ($M = 62\,M_\odot$): $m_2 r_{\mathrm{peak}} = 7.78 \times 10^9$, giving $\log_{10}(\delta\omega/\omega) \approx -3.4 \times 10^9$.

2. *Perturbation-equation correction* (parametric estimate): $\delta\omega/\omega \sim \mathcal{O}(1) \cdot c_2(\omega/\Lambda)^2$, where $c_2 = 13/60$ and $\mathcal{O}(1)$ is an unknown dimensionless coefficient depending on the open problem Gap G1 (computation of $\delta\Theta^{(C)}_{\mu\nu}$ on the Schwarzschild background). For GW150914: $\omega/\Lambda \approx 3.4 \times 10^{-10}$, giving $\delta\omega/\omega \sim 10^{-20}$ up to the $\mathcal{O}(1)$ factor.

Contribution (2) dominates by $\sim 10^{3\times 10^9}$ orders of magnitude. Both are ≥ 15 orders below LIGO sensitivity ($\sim 10^{-1}$). Results for observed black holes are given in Table 5. Numerical values are computed in the Stelle approximation ($m_2^{\mathrm{Stelle}} = \Lambda\sqrt{60/13} \approx 2.148\,\Lambda$); for the exact propagator zero (12) ($m_2 = 1.554\,\Lambda$ at $n = 1$) the values of $m_2 r_{\mathrm{peak}}$ decrease by $1.554/2.148 \approx 0.72$, shifting $\log_{10}(\delta\omega/\omega)$ by ~ 0.14 — within the order-of-magnitude accuracy of the estimate. At $\xi = 1/6$ the scalar mode decouples and $h(r) = 1 - (4/3)\,e^{-m_2 r}$; the table is given for $\xi = 0$ (both Yukawa modes) for generality.

Quantum corrections dominate classical ones. The one-loop quantum correction to QNM frequencies is $\delta\omega_{\mathrm{quantum}}/\omega \sim (l_P/r_s)^2 c_{\log} \sim 10^{-78}$ for $10\,M_\odot$ ($c_{\log} = 37/24$). The classical SCT metric correction: $\delta\omega_{\mathrm{SCT}}/\omega \sim e^{-10^9} \ll 10^{-78}$. Quantum corrections dominate by $\sim 10^{10^9 - 78}$ orders. The exponential suppression of the classical correction is independently confirmed in local quadratic gravity by Antoniou, Gualtieri and Pani [**? ?**].

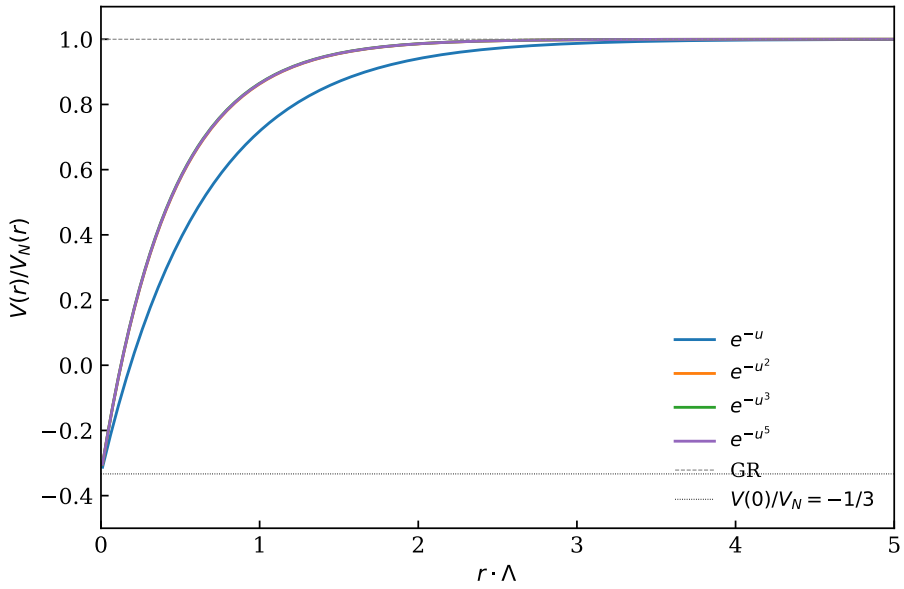

Figure 3: Modified Newtonian potential $V(r)/V_N(r)$ at $\xi = 1/6$ for three cutoff functions ($n = 1, 2, 5$) and the GR limit. All cutoffs give $V(0)/V_N = -1/3$ (repulsive origin). The spread narrows for $n \geq 2$.

Table 5: SCT QNM frequency shifts for observed black holes ($l = 2$, $n = 0$).

Object	$M/M_\odot$	$m_2 r_{\rm peak}$	$\log_{10}(\delta\omega/\omega)_{\rm total}$
$10\,M_\odot$	10	1.3×10^9	-17.9
GW150914	62	7.8×10^9	-19.5
GW190521	142	1.8×10^{10}	-20.3
Sgr A*	4.15×10^6	5.2×10^{14}	-29.2
M87*	6.5×10^9	8.2×10^{17}	-35.5

Mode stability. For odd (axial) parity, an analytic theorem holds: the full Regge–Wheeler potential $V_{\rm odd}^{\rm SCT} = (f/r^2)[\ell(\ell+1) - 3(1-f) + r_s h'(r)]$ satisfies $V > 3f/r^2 > 0$ for all $r > r_H$, $\ell \geq 2$, using $h' > 0$ and $0 < f < 1$ outside the horizon. By the Kay–Wald theorem [**?**] this excludes growing modes.

Tidal Love numbers. In GR, $k_2 = 0$ exactly for black holes [**?**]. In SCT, $k_2 \neq 0$ (qualitative difference from GR), but $|k_2| \sim \exp(-m_2 r_s)$: unmeasurable for astrophysical objects.

Gravitational echoes. The SCT potential has exactly *one* external maximum for all $M > M_{\rm min}$. No cavity (double-barrier) structure forms; gravitational echoes are structurally impossible.

Superradiance. For astrophysical BHs: $\alpha = m_2 M \gg 1$, no quasi-bound states. The boundary $\alpha = 1$ at $m_2 = 1.554\,\Lambda$ and $\Lambda = 3.53$ meV gives $M_{\alpha=1} = 1/(m_2 G) \approx 5 \times 10^{-8}\,M_\odot$; the lower bound $M_{\rm min} \approx 1.4 \times 10^{-8}\,M_\odot$ is the minimum mass for which a horizon exists [**?**]. In the window $M_{\rm min} < M < M_{\alpha=1}$, a horizon exists with $\alpha < 1$;

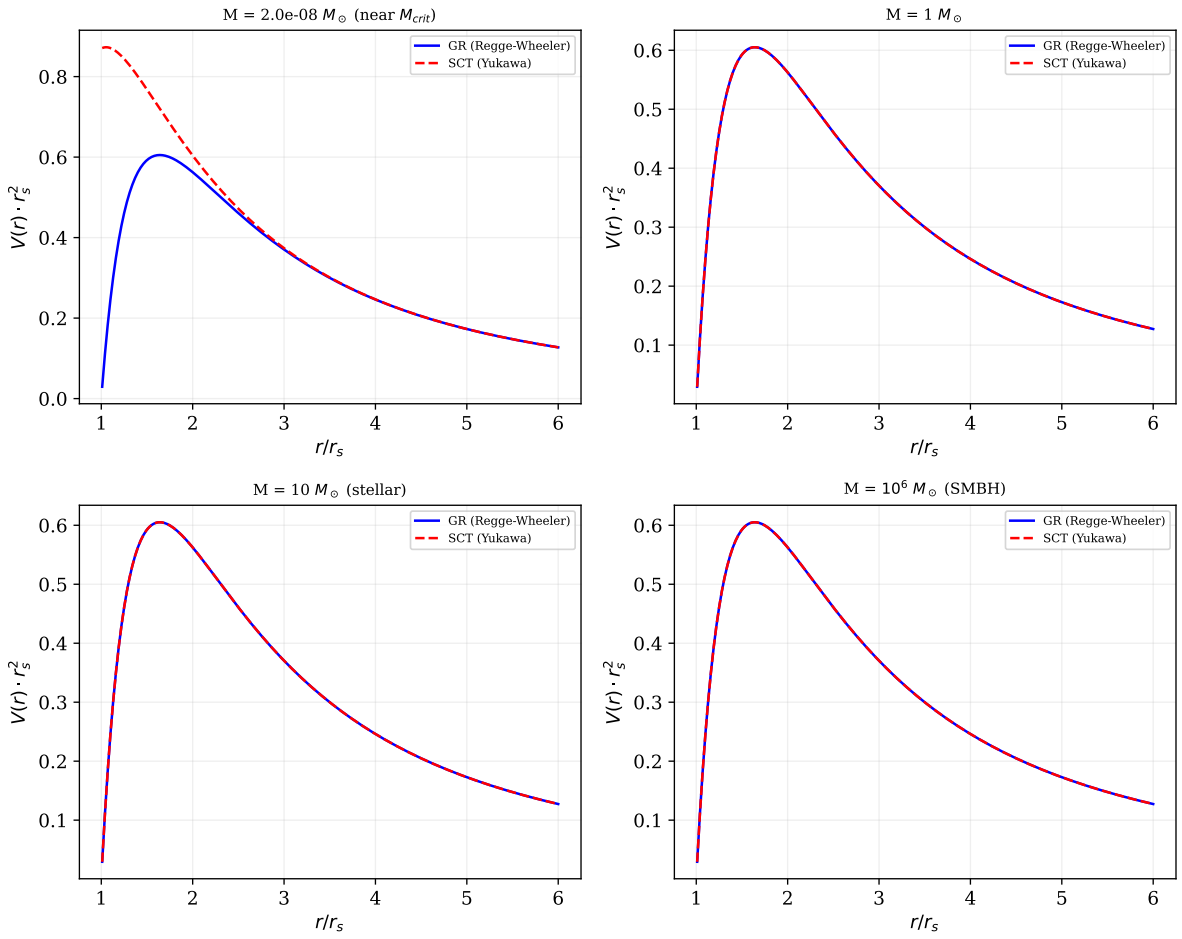

Figure 4: Regge–Wheeler potentials ($l = 2$): GR (blue) vs. SCT (red dashed) at four masses. Top left: near M_{crit}, modification is $O(1)$. Other panels: modification is exponentially suppressed and invisible.

without the fakeon prescription, a standard ghost would trigger superradiant instability. The fakeon projects out on-shell states and prevents cloud formation.

Kerr and Reissner–Nordström. For Kerr at $a/M = 0.998$, the dominant correction rises to $\sim 10^{-17}$ (from $\sim 10^{-20}$ at $a = 0$), still unmeasurable. For extremal Reissner–Nordström ($Q/M \to 1$): $\sim 10^{-18}$.

QNM bounds on Λ. In the Cardoso et al. parametrization [**?**], the Yukawa correction maps to $\alpha_j = 0$ for all j (beyond-all-orders in r_H/r). The formal LIGO ringdown bound: $\Lambda_{\text{QNM}} \sim 2.2 \times 10^{-12}$ eV, nine orders weaker than $\Lambda_{\text{Eöt-Wash}} > 3.53$ meV.

Summary of Λ bounds. Different channels span 21 orders of magnitude (Table 6).

5.3 Other null predictions

Beyond QNMs, the following observables are indistinguishable from GR:

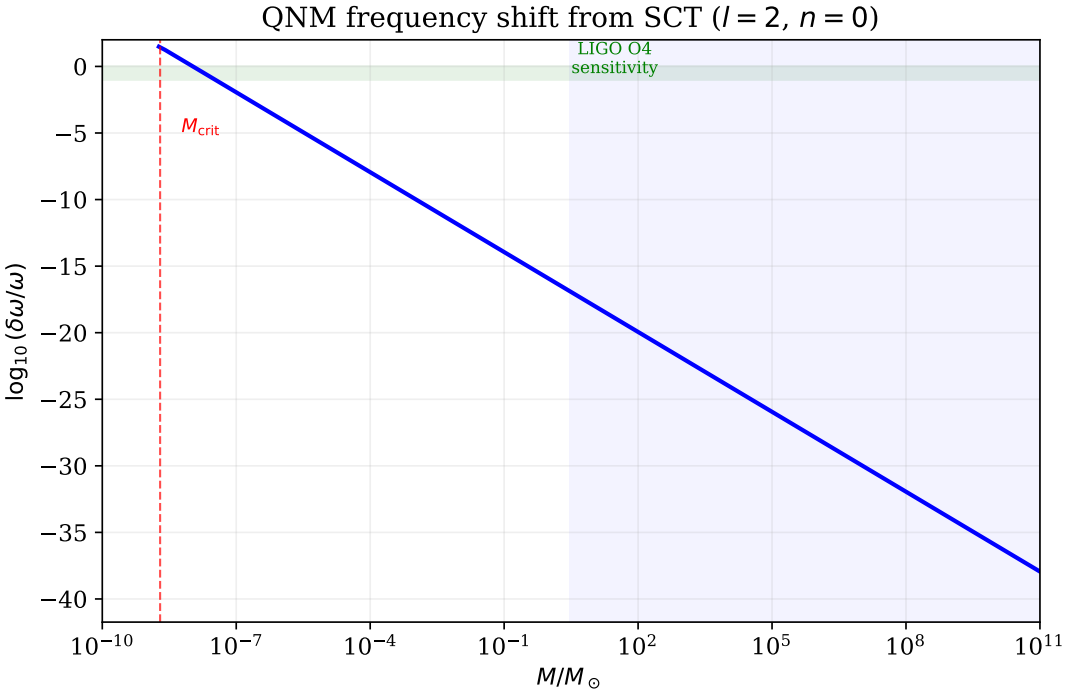

Figure 5: Total QNM frequency shift $\delta\omega/\omega$ vs. BH mass ($l = 2$, $n = 0$). For small masses ($M \lesssim M_{\rm min}$): metric modification $\sim e^{-m_2 r_{\rm peak}}$ dominates. For astrophysical masses ($M \gtrsim 1\,M_\odot$): perturbation-equation correction $\sim c_2(\omega/\Lambda)^2$ dominates. Green band: LIGO O4 sensitivity.

- Neutron star structure (unmodified TOV equation),
- Late-time cosmology ($\delta H^2/H^2 \sim 10^{-64}$; [**?**]).

5.4 Swampland tension

The SCT scalaron potential (if the scalaron existed) would violate the refined de Sitter Swampland conjecture [**?**] at $\mathcal{O}(1)$ parameter values. The curvature condition has a hard ceiling $\eta_{\rm min} = -1/3$, which cannot satisfy the Swampland parameter $\tilde{c} \sim 1$.

Since $\xi = 1/6$ eliminates the scalaron entirely, this tension is moot for the standard spectral action: there is no scalar potential to test against the conjecture. Confirmation of pure Starobinsky inflation by CMB-S4 or LiteBIRD [**?**] would increase the tension between the Swampland programme and R^2-type models in general.

6 Comparison with competing programs

6.1 Programs compared

We compare SCT with five quantum gravity programs: *Loop Quantum Gravity* (LQG) [**?** **?**], based on non-perturbative canonical quantization with spin-network states; *Asymptotic Safety* (AS) [**?**], based on the existence of a non-Gaussian UV fixed point of the

Table 6: Bounds on the cutoff scale Λ from different channels.

Channel	$\Lambda_{\min}$	Source
GW dispersion (GWTC-3)	> 8.50 meV	[**?**]
Eöt-Wash (dedicated)	$\mathbf{> 3.53}$ **meV**	this work
Eöt-Wash (Stelle)	> 2.57 meV	[**?**], superseded
Solar system (Cassini)	> 2.38 meV	[**?**], superseded
LIGO ringdown (QNM)	$> 2.2 \times 10^{-12}$ eV	this work
BH shadow (EHT)	$\sim 10^{-30}$ eV	this work

gravitational RG flow; *Causal Dynamical Triangulations* (CDT) [**?**], a lattice approach with a causal constraint on the path integral; *string theory* [**?**], based on one-dimensional extended objects replacing point particles; and *Infinite Derivative Gravity* (IDG) [**?** **?**], which modifies the graviton propagator with an entire-function form factor to achieve ghost-freedom. We do not include Causal Set Theory [**?**] as a separate entry: it does not by itself produce the quantitative predictions listed in the comparison axes, though the CJ bridge formula [**?**] connects SCT to causal-set observables.

6.2 Comparison table

Table 7 presents the comparison across nine quantitative axes. Each cell contains the best available numerical value (or status assessment) from the primary literature.

Table 7: Cross-program comparison. Abbreviations: n.c. = not computed, m.d. = model-dependent, n.p. = not predicted. References are given in the text.

Axis	SCT	LQG	AS	CDT	String	IDG
d_S(UV)[a]	method-dep.	~ 2	2 (exact)	1.80 ± 0.25	m.d.	2
$c_{\log}$	$+37/24$	$-1/2$	0 or π/g_*	n.c.	charge-dep.	no log
Singularity	unresolved[b]	bounce	$G \to 0$	n.c.	fuzzball	resolved
n_s, r	excluded	$r = 0.07$–0.17 [**?**]	$r \approx 0.003$	n.c.	landscape	$n_s = 1{-}2/N$
Dispersion	$\omega = k^c$	m.d.	n.c.	n.c.	unmod.	unmod.
$\gamma_{\rm PPN}$	1	1	1	n.c.	1	1
UV prop.	entire[d]	spinfoam	power-law	lattice	string-scale	Gaussian
$\Lambda_{\rm cc}$	n.p.	n.p.	n.p.	> 0 req.	10^{500}	n.p.
Matter	$\alpha_C = 13/120$	free	FP bounds	n.c.	landscape	minimal

[a] SCT value depends on definition. In the Mittag-Leffler method, d_S passes through ≈ 2 near the ghost scale, but the flow is non-monotonic (oscillatory), unlike the monotonic $4 \to 2$ transition in CDT/AS/LQG. Under the HK definition: $d_S = 4$; ASZ: $d_S = 0$.

[b] Yukawa potential gives $V(0)/V_N = -1/3$; the full nonlocal potential diverges as $r \to 0$ (one loop).

[c] One-loop result.

[d] Entire function of order 1; the fakeon prescription for countably many complex poles requires a convergence proof.

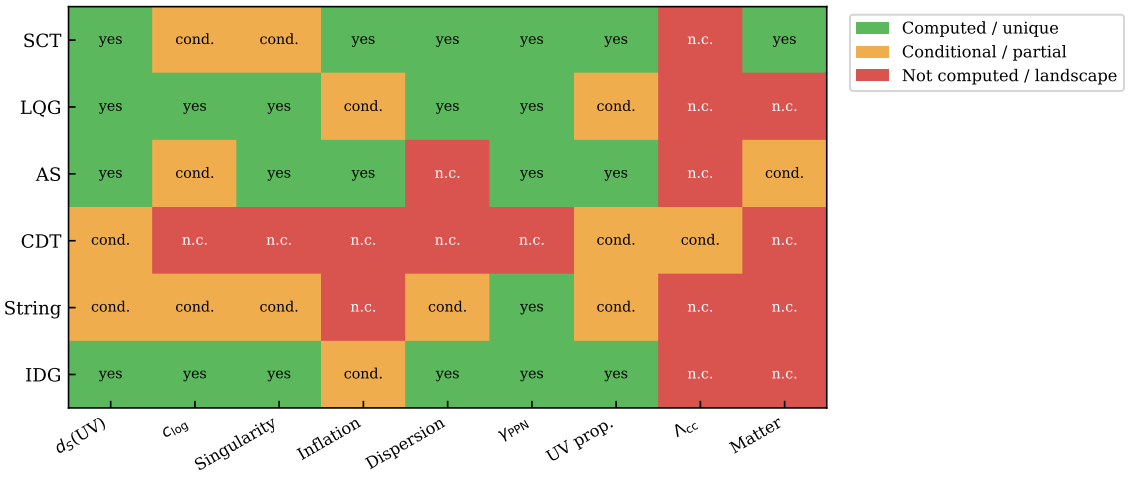

Figure 6: Prediction status across six quantum gravity programs and nine axes. Green: computed or unique prediction. Yellow: conditional or partial. Red: not computed or landscape-dependent. SCT has computed entries on 8/9 axes; CDT has computed entries on 2/9.

6.3 Discriminating observables

Three axes yield predictions that are mutually incompatible across programs:

(1) $c_{\log}$**.** SCT: $+37/24$. LQG: $-1/2$. Opposite sign. AS: definition-dependent. IDG: no logarithmic correction. A measurement of $c_{\log}$ (e.g., through black hole area quantization signatures in LISA data [**?**]) would sharply discriminate between programs.

(2) **UV propagator.** SCT: entire function of order 1. IDG: Gaussian $e^{-k^2/M^2}/k^2$. AS: power-law $G(k) \to g_*/k^2$. LQG: discrete spinfoam amplitude. These are four qualitatively distinct analytic structures.

(3) **Matter coupling.** SCT: $\alpha_C = 13/120$, determined by the SM particle content alone. AS: the non-Gaussian fixed point constrains the number of matter fields but does not fix the coupling coefficient. LQG, string, IDG: matter coupling is a free input. SCT is the only program in this comparison where the zero-momentum gravitational coupling coefficient $\alpha_C(0) = 13/120$ is determined by the SM particle content alone, without additional free parameters.

6.4 SCT and asymptotic safety

SCT and AS share identical matter one-loop form factors: the Codello–Zanusso basis function $f_C(x) = 1/(12x) + (\varphi - 1)/(2x^2)$ [**?**] coincides with $h_C^{(0)}(x)$ (4). This identity holds for any cutoff function (it is a property of the heat kernel, not of the RG scheme).

The first divergence occurs at the graviton loop level. Including graviton and ghost contributions, the full one-loop AS Weyl coefficient is [**?**]

$$\alpha_C^{\mathrm{AS}} = \frac{13}{120} + \frac{7}{20} = \frac{11}{24} \approx 0.458 = 4.23\, \alpha_C^{\mathrm{SCT}}. \tag{20}$$

The comparison (20) does *not* compare like with like: α_C^{SCT} sums only over matter loops (the spectral action is a trace over matter fields), whereas α_C^{AS} includes also graviton and Faddeev–Popov ghost contributions. The agreement of the matter part (13/120) is a nontrivial cross-check, not a prediction of a new effect. These graviton-loop contributions are absent in the SCT spectral action (which sums over matter fields only).

The UV universality classes differ: SCT form factors are entire functions (the propagator saturates at a finite constant in the deep UV), while AS predicts power-law running with anomalous dimension $\eta_N = -2$ at the fixed point [**?**].

6.5 Universal features

The spectral dimension $d_S \to 2$ in the UV is obtained by SCT, LQG, AS, and IDG. CDT gives $d_S = 1.80 \pm 0.25$ (original measurement by [**?**], within 1σ of 2). This near-universality across disparate approaches has been noted by [**?**].

All six programs predict $\gamma_{\mathrm{PPN}} = 1$ at solar system scales. No program predicts a specific value for the cosmological constant.

7 Falsification criteria

Table 8 lists observations that would contradict specific SCT predictions.

Table 8: Falsification criteria. Each row states an observation that would contradict the indicated SCT prediction, the experiment that could make the observation, and the approximate timeline.

Observation	Implication for SCT	Experiment	Timeline
Scalar GW polarization detected	$\xi \neq 1/6$; standard spectral triple insufficient	ET/CE network	2035+
$c_{\log} < 0$	App. B derivation wrong; LQG prediction favored	theoretical[e]	—
GW birefringence detected	Parity violation in gravity; discrete structure (LQG-type)	Fermi-LAT, CTA	ongoing
Short-range deviation at $r > 56\ \mu$m	$\Lambda < 3.53$ meV; phenomenology requires revision	Torsion balance	2030s
$r \approx 0.003$ from R^2 inflation	$\alpha_R \neq 0$, hence $\xi \neq 1/6$ or BSM	CMB-S4, LiteBIRD	2028–32

[e]The criterion is theoretical: $c_{\log}$ is falsified by an independent computation of the sign in a competing program, not by direct experimental measurement (for astrophysical BHs, $\ln(A/\ell_P^2) \sim 10^2$, which is unmeasurable at current precision).

We emphasize that detection of a scalar GW polarization would not falsify SCT as a framework, but would require replacing the standard spectral triple with a BSM extension

in which $\xi \neq 1/6$.

8 Discussion

SCT is a one-loop gravitational effective field theory [**?**], valid through two loops under the D^2-quantization chirality theorem [**?**]. At three loops, the existence of three independent quartic Weyl invariants versus one spectral-function parameter creates a structural overdetermination [**?**]. The theory is therefore best characterized as an EFT valid through $L = 2$, not as a UV-complete quantum gravity theory.

The cutoff function f introduces an infinite-dimensional ambiguity in the form factors, but the predictions testable at macroscopic scales with current technology (PPN parameters, GW speed, absence of scalar mode) all lie in the cutoff-independent sector. We note that while the ratio $\alpha_C = 13/120$ is f-independent, the absolute magnitude of the C^2 term in the action involves the moment $f_4 = \int_0^\infty f(u)\, u\, \mathrm{d}u$, which depends on f. The cutoff-dependent predictions (effective masses, potential shape, spectral dimension flow) are bounded but not uniquely determined. Off-shell quantities (propagator zeros, effective masses) are additionally gauge-dependent; the on-shell predictions (scattering amplitudes, PPN parameters) are gauge-invariant.

The spectral action (1) is formulated in Euclidean signature. The continuation to Lorentzian signature follows Barvinsky and Vilkovisky [**?**] via Wick rotation of the form factor arguments; the fakeon prescription [**?**] operates in Lorentzian signature. A fully non-perturbative Lorentzian formulation of the spectral action remains an open problem.

The fakeon prescription resolves the unitarity problem at one loop. The extension to all orders requires proving that Anselmi's finite-threshold argument [**?**] generalizes to the countably infinite pole set of the SCT propagator. This remains an open problem.

Among the six programs compared, SCT is the only one where the matter coupling coefficient α_C is fully determined by the Standard Model particle content. This is a consequence of the spectral action principle, which derives the gravitational effective action from the spectrum of the Dirac operator coupled to matter.

9 Conclusions

We have cataloged the predictions of Spectral Causal Theory and classified them by their dependence on the cutoff function f. The results are:

(1) Two unconditional predictions: $\alpha_C = 13/120$ and $c_1/c_2 = -1/3$ at $\xi = 1/6$ (Table 1). Two established: absence of the scalar mode at $\xi = 1/6$ and exclusion of Starobinsky inflation. Three conditional: PPN parameters and $c_T = c$ (conditional on the generalized fakeon prescription and Wick rotation) and $c_{\log} > 0$ (conditional on the Sen formula and field content; value 37/24 for SM, 8/5 for SM+ν_R).

(2) Cutoff-dependent predictions (Table 4): the fakeon mass $m_2/\Lambda = 1.554$ at $n = 1$ (rigorously justified cutoff); results for $n \geq 2$ are formal extrapolations (see the caveat in the table).

(3) The massless graviton ($z = 0$) has dispersion $\omega = k$ at one-loop level (Euclidean derivation), with no birefringence. QNM corrections on curved backgrounds are $\sim \mathcal{O}(1) \cdot c_2(\omega/\Lambda)^2$ — a parametric estimate with an unknown $\mathcal{O}(1)$ factor (Gap G1 open).

(4) Three discriminating observables: the *sign* of $c_{\log}$ (not the value), UV propagator analytic structure, and matter coupling coefficient.

(5) Five falsification criteria stated (Table 8).

(6) Within the fakeon prescription, SCT is consistent with all current observational data. Modifications to GR are suppressed at macroscopic scales: power-law ($\sim \mathcal{O}(1) \cdot c_2(\omega/\Lambda)^2 \sim 10^{-20}$ up to the $\mathcal{O}(1)$ factor for the perturbation-equation correction) and exponentially ($\sim e^{-m_2 r_s}$ for the metric modification).

(7) Modal stability of SCT-Schwarzschild proven analytically for odd parity ($V > 3f/r^2 > 0$, $\ell \geq 2$). Tidal Love numbers $k_2 \neq 0$ (qualitative GR difference), gravitational echoes structurally impossible (single-barrier potential), superradiant instability prevented by the fakeon prescription (Table 5).

The strongest discriminant between SCT and competing programs is the *sign* of the logarithmic black hole entropy correction: $c_{\log} > 0$ (SCT, for any field content with the dominant graviton contribution) versus $c_{\log} < 0$ (LQG, $-1/2$ or $-3/2$ depending on the method).

A Cutoff function scan

The generalized master function for $f(u) = e^{-u^n}$ is

$$\varphi_n(x) = \int_0^1 \exp\bigl(-[\alpha(1-\alpha)\,x]^n\bigr)\,\mathrm{d}\alpha. \tag{21}$$

At $x = 0$: $\varphi_n(0) = 1$ for all n (the integrand reduces to 1). For $n = 1$: $\varphi_1'(0) = -1/6$. For $n \geq 2$: $\varphi_n'(0) = 0$ because the chain rule produces a factor x^{n-1} that vanishes at $x = 0$. The leading correction is then set by the n-th derivative: $\varphi_n(x) = 1 + \mathcal{O}(x^n)$.

The first positive real zero z_0 of $\Pi_{\mathrm{TT}}(z)$ was located using Brent's method (SciPy `brentq`) after a sign-change scan over $z \in [0.1, 20]$ with step size 0.05. All computations used 50-digit arithmetic (mpmath). The $n = 1$ result $z_0 = 2.4148$ was cross-checked against the canonical SCT codebase [**?**], with agreement to all 50 digits.

B Derivation of $c_{\log} = 37/24$

The one-loop logarithmic correction to the Bekenstein–Hawking entropy for a non-extremal Schwarzschild black hole is given by the Sen formula [**?**]:

$$c_{\log} = \frac{1}{180}\bigl[2\,N_s + 7\,N_F - 26\,N_V + 424\bigr], \tag{22}$$

where N_s is the number of real scalars, N_F the number of Dirac fermions, N_V the number of gauge vectors, and $+424$ is the graviton contribution [**?**]. Sen's convention uses $\ln a_H$ where $A_H \sim a_H^2$; our $c_{\log}$ is the coefficient of $\ln(A_H/\ell_P^2)$, hence the prefactor $1/180 = 1/(2 \times 90)$. The coefficient -26 per vector arises from the proper vector determinant ($+62$) minus two Faddeev–Popov ghosts ($2 \times 44 = 88$), giving $62 - 88 = -26$. The fermion coefficient is $+7$ per Dirac fermion (not $+7/2$ per Weyl). The formula uses zeta-function regularisation on the Euclidean Schwarzschild instanton with Dirichlet boundary conditions at the horizon.

For the Standard Model field content ($N_s = 4$, $N_F = 22.5$, $N_V = 12$):

Field	Coefficient	Contribution
Scalars	2×4	$+8$
Fermions	7×22.5	$+157.5$
Vectors	-26×12	-312
Graviton		$+424$
Total		277.5

Therefore

$$\boxed{c_{\log} = \frac{277.5}{180} = \frac{37}{24} \approx 1.542\,.} \tag{23}$$

The matter contribution alone is $-146.5/180 < 0$ (dominated by vector Faddeev–Popov ghosts); the graviton term $+424$ makes the total positive.

Remark B.1 (Cross-checks). Pure gravity ($N_s = N_F = N_V = 0$): $c_{\log}^{\text{pure}} = 424/180 = 106/45 \approx 2.36$, consistent with Sen's $C_{\text{local}} = 212/45$ after the $\ln a_H \to \ln A_H$ conversion [**?**]. The computation has been verified by exact rational arithmetic (Fraction$(555, 2)/180 =$ Fraction$(37, 24)$) and agrees with the conformal anomaly approach using the coefficients $a = 1/360$, $c = 1/120$ per real scalar [**?**].

This gives the local heat-kernel contribution; ensemble-dependent zero-mode corrections (Sen [**?**], Section 4.2: $\delta c_{\log} \in [-3/4,\, 0]$) shift $c_{\log}$ by at most $-3/4$ without changing its sign. The sign of $c_{\log}$ is positive for the SM, opposite to the LQG prediction ($c_{\log}^{\text{LQG}} = -1/2$ or $-3/2$ [**? ?**]).

Acknowledgments

We thank Igor Shnyukov for collaboration on "Weyl curvature from the Hasse diagram" [**?**].

Data availability

All numerical data, computational scripts, and verification results are available in the SCT Theory repository [**?**]. The comparison table data are stored in machine-readable JSON format.

Declarations

Conflict of interest

The author declares no conflict of interest.

Use of AI tools

Large language models (Claude, Anthropic) were used for code generation and numerical verification scripting. All mathematical derivations, physical arguments, and scientific conclusions were formulated and verified by the author. The AI-generated code was independently validated against analytical results at 100-digit precision.

References